

We are IntechOpen, the world's leading publisher of Open Access books Built by scientists, for scientists

6,900

Open access books available

186,000

International authors and editors

200M

Downloads

Our authors are among the

154

Countries delivered to

TOP 1%

most cited scientists

12.2%

Contributors from top 500 universities



WEB OF SCIENCE™

Selection of our books indexed in the Book Citation Index
in Web of Science™ Core Collection (BKCI)

Interested in publishing with us?
Contact book.department@intechopen.com

Numbers displayed above are based on latest data collected.
For more information visit www.intechopen.com



Optical Effects Connected with Coherent Polarized Light Propagation Through a Step-Index Fiber

Maxim Bolshakov, Alexander Ershov and Natalia Kundikova
*Joint Nonlinear Optics Laboratory of the Electrophysics Institute
and South Ural State University
Russia*

1. Introduction

Spin-orbital interaction of a photon manifests itself in two effects. The first one is the influence of the trajectory on the light polarization. The second one is the influence of the polarization on the trajectory of light. The influence of the trajectory on the light polarization has been investigated theoretically (Chiao & Wu, 1986; Rytov, 1938; Vladimirskii, 1941) and the change in the azimuth of linearly polarized light has been observed experimentally under light propagation through a helical (coiled into a spiral) single mode optical fiber (Tomita & Chiao, 1986). The influence of light polarization on trajectory was demonstrated for the first time under total internal reflection. It was shown that reflected rays suffer a longitudinal shift for the linearly polarized light (Goos & Hanchen, 1947; 1949; Picht, 1929) and transverse shift for the circularly polarized light (Fedorov, 1955; Imbert, 1972). The value of the shifts is on the order of the light wavelength and depends on the state of light polarization. All mentioned effects have been investigated independently till 1990. The influence of the trajectory on polarization and the influence of the polarization on the trajectory were considered as mutually inverse effects for the first time by Zel'dovich and Liberman in 1990 (Zel'dovich & Liberman, 1990). The interpretation of these effects in terms of quantum mechanics as an interaction between the orbital momentum of photon and its spin (polarization) has been done by Zeldovich, Dooghin, Kundikova and Liberman in 1991 (Doogin et al., 1991). This interpretation was based on prediction and experimental investigation of optical Magnus effect. The effect manifests itself as speckle pattern rotation of circular polarized light transmitted through a multimode step-index fiber under circular polarization sign change (Doogin et al., 1992; 1991).

The chapter describes the results obtained in our laboratory, namely the results of investigation of optical effects connected with coherent polarized light propagation through a step-index fiber. This chapter is based on published results, but some recent results are added. The chapter is organized in the following way. The first section is devoted to the theoretical description of coherent polarized light wave propagation through a multimode step-index fiber. The approximation of weak guiding modes is used. The results of the next sections are based on the first section. The second section presents the results of the theoretical prediction and the experimental investigation of the isolated wave front dislocation formation (Darsht et al., 1995). The optical Magnus effect (Doogin et al., 1992) and its peculiarity in a

few modes fiber are discussed in the third section. It also presents the results of computer simulation and the experimental results. The optical Magnus effect is observed under the switch of the circular polarization sign. The influence of light polarization on the speckle pattern of the polarized light transmitted through a multimode optical fiber will be described in the fourth section (Bolshakov & Kundikova, 2003; Bolshakov et al., 2006). The influence of external magnetic field on the speckle pattern behavior is considered in the fifth section, as well as the results of computer modeling and the experimental results. (Anikeev et al., 2001; Ardasheva et al., 2002; Baranova & Zel'dovich, 1994; Darst et al., 1994). The sixth section deals with the applications results for fiber sensors (Bolshakov et al., 2008; 2011).

2. Theoretical description of coherent polarized light wave propagation through a multimode step-index fiber

Let's consider propagation of polarized light in an axial symmetric optical fiber with the following refractive index profile:

$$n^2(R) = n_{\text{co}}^2 [1 - 2\Delta f(R)], \quad (1)$$

where

$$\Delta = \frac{1}{2} \left(1 - \frac{n_{\text{cl}}^2}{n_{\text{co}}^2} \right), \quad (2)$$

and in the approximation of weakly directing waveguide

$$\Delta \approx \frac{n_{\text{co}} - n_{\text{cl}}}{n_{\text{co}}}. \quad (3)$$

The function $f(R)$ looks like the following:

$$\begin{aligned} f(R) &= 0, & R &= r/\rho < 1, \\ f(R) &= 1, & R &= r/\rho > 1, \end{aligned} \quad (4)$$

and

$$\begin{aligned} n(r) &= n_{\text{co}}, & r/\rho &< 1, \\ n(r) &= n_{\text{cl}}, & r/\rho &> 1. \end{aligned} \quad (5)$$

Here $r = |\mathbf{r}|$, $(x, y) = \mathbf{r}$ are the transverse coordinates, ρ is the radius of the fiber core, n_{co} and n_{cl} are the refractive indexes of the core and the cladding respectively. In the approach of weakly directing waveguide the requirements of symmetry allow to write down four polarization modes in the following form for any orbital angular momentum m ($m \geq 0$) and radial quantum number N (Snyder & Love, 1984):

$$\begin{aligned} \mathbf{e}_{m,N}^{(1)}(r, \varphi) &= [\cos(m\varphi) \mathbf{e}_x - \sin(m\varphi) \mathbf{e}_y] \cdot F_{m,N}(r), \\ \mathbf{e}_{m,N}^{(2)}(r, \varphi) &= [\cos(m\varphi) \mathbf{e}_x + \sin(m\varphi) \mathbf{e}_y] \cdot F_{m,N}(r), \\ \mathbf{e}_{m,N}^{(3)}(r, \varphi) &= [\sin(m\varphi) \mathbf{e}_x + \cos(m\varphi) \mathbf{e}_y] \cdot F_{m,N}(r), \\ \mathbf{e}_{m,N}^{(4)}(r, \varphi) &= [\sin(m\varphi) \mathbf{e}_x - \cos(m\varphi) \mathbf{e}_y] \cdot F_{m,N}(r). \end{aligned} \quad (6)$$

Here $\mathbf{e}_x, \mathbf{e}_y$ are the eigenvectors, $x = r \cdot \cos \varphi$, $y = r \cdot \sin \varphi$. The radial distribution function $F_{m,N}(R)$ looks like:

$$F_{m,N}(R) = \frac{J_m(U_N R)}{J_m(U_N)}, \quad R = r/\rho < 1,$$

$$F_{m,N}(R) = \frac{K_m(W_N R)}{K_m(W_N)}, \quad R = r/\rho > 1, \quad (7)$$

where J_m and K_m are Bessel and McDonald functions accordingly, quantities U_N and W_N for each value m are determined from the equation:

$$U_N \frac{J_{m+1}(U_N)}{J_m(U_N)} = W_N \frac{K_{m+1}(W_N)}{K_m(W_N)}, \quad (8)$$

where $V^2 = W_N^2 + U_N^2$, $V = \rho k \sqrt{2n_{co}(n_{co} - n_{cl})}$, $k = 2\pi/\lambda$, λ is the wavelength of light in the air. In the scalar approach all modes propagate with an equal velocity, determined by the propagation constant $\beta_{m,N}$:

$$\beta_{m,N} = \frac{V}{\rho(2\Delta)^{1/2}} \left\{ 1 - 2\Delta \frac{U_N^2}{V^2} \right\}^{1/2}. \quad (9)$$

The influence of the state of polarization of each of the four modes on its propagation velocity is taken into account by the introduction of the polarization corrections $\delta\beta_{m,N}^{(j)}$ to the propagation constants. The polarization corrections are determined as follows:

$$\begin{aligned} \delta\beta_{0,N}^{(1)} &= \delta\beta_{0,N}^{(3)} = \delta\beta_{0,N}^{(2)} = \delta\beta_{0,N}^{(4)} = I_1, \\ \delta\beta_{1,N}^{(1)} &= \delta\beta_{1,N}^{(3)} = I_1 - I_2, \\ \delta\beta_{1,N}^{(2)} &= 2(I_1 + I_2), \\ \delta\beta_{1,N}^{(4)} &= 0, \\ \delta\beta_{m,N}^{(1)} &= \delta\beta_{m,N}^{(3)} = I_1 - I_2, \\ \delta\beta_{m,N}^{(2)} &= \delta\beta_{m,N}^{(4)} = I_1 + I_2. \end{aligned} \quad (10)$$

Here

$$I_1 = I_1(m, N) = \frac{(2\Delta)^{3/2} \int_0^\infty R F_{m,N} \left(\frac{dF_{m,N}}{dR} \right) \delta(R-1) dR}{4\rho V \int_0^\infty R F_{m,N}^2 dR},$$

$$I_2 = I_2(m, N) = m \frac{(2\Delta)^{3/2} \int_0^\infty F_{m,N}^2 \delta(R-1) dR}{4\rho V \int_0^\infty R F_{m,N}^2 dR}. \quad (11)$$

If the fiber has a step like refractive index profile, the expressions will be the following:

$$I_1(0, N) = -\frac{(2\Delta)^{3/2} W_N U_N^2 K_0(W_N)}{2\rho V^3 K_1(W_N)},$$

$$I_1(m, N) = -\frac{(2\Delta)^{3/2} W_N U_N^2 K_{m-1}(W_N) + K_{m+1}(W_N)}{4\rho V^3 K_{m-1}(W_N) K_{m+1}(W_N)} K_m(W_N),$$

$$I_2(m, N) = m I_{20}(m, N) = m \frac{(2\Delta)^{3/2} U_N^2 K_m^2(W_N)}{2\rho V^3 K_{m-1}(W_N) K_{m+1}(W_N)}. \quad (12)$$

Taking into account Eq. (12) let us obtain the following expressions for the polarization corrections to the propagation constants in the case of a fiber with a step like refractive index profile:

$$\begin{aligned}
 \delta\beta_{0,N}^{(1)} &= \delta\beta_{0,N}^{(3)} = \delta\beta_{0,N}^{(2)} = \delta\beta_{0,N}^{(4)} = -\frac{(2\Delta)^{3/2} W_N U_N^2 K_0(W_N)}{2\rho V^3 K_1(W_N)}, \\
 \delta\beta_{1,N}^{(1)} &= \delta\beta_{1,N}^{(3)} = -\frac{(2\Delta)^{3/2} W_N U_N^2 K_1(W_N)}{2\rho V^3 K_0(W_N)}, \\
 \delta\beta_{1,N}^{(2)} &= -\frac{(2\Delta)^{3/2} W_N U_N^2 K_1(W_N)}{\rho V^3 K_2(W_N)}, \\
 \delta\beta_{1,N}^{(4)} &= 0, \\
 \delta\beta_{m,N}^{(1)} &= \delta\beta_{m,N}^{(3)} = -\frac{(2\Delta)^{3/2} W_N U_N^2 K_m(W_N)}{2\rho V^3 K_{m-1}(W_N)}, \\
 \delta\beta_{m,N}^{(2)} &= \delta\beta_{m,N}^{(4)} = -\frac{(2\Delta)^{3/2} W_N U_N^2 K_m(W_N)}{2\rho V^3 K_{m+1}(W_N)}.
 \end{aligned} \tag{13}$$

As $\delta\beta_{m,N}^{(1)} = \delta\beta_{m,N}^{(3)}$ for all values of m and $\delta\beta_{m,N}^{(2)} = \delta\beta_{m,N}^{(4)}$ for all values $m \neq 1$, any linear combinations of the modes $\mathbf{e}_{m,N}^{(1)}$ and $\mathbf{e}_{m,N}^{(3)}$ for all values m and any linear combinations of the modes $\mathbf{e}_{m,N}^{(2)}$ and $\mathbf{e}_{m,N}^{(4)}$ in the case $m \neq 1$ will be also eigenmodes. It is easy to show that combinations of the modes $\mathbf{e}_{m,N}^{(1)} \pm i\mathbf{e}_{m,N}^{(3)}$ and $\mathbf{e}_{m,N}^{(2)} \pm i\mathbf{e}_{m,N}^{(4)}$ ($i = \sqrt{-1}$) represent the modes with the homogeneous on the section of the fiber circular polarization $\mathbf{e}_x + i\sigma\mathbf{e}_y$. Here $\sigma = +1$ for light with the right circular polarization and $\sigma = -1$ for light with the left circular polarization. These new modes are those:

$$\begin{aligned}
 \mathbf{e}_{+,m,N}^+ &= \mathbf{e}_{m,N}^{(1)}(r,\varphi) + i\mathbf{e}_{m,N}^{(3)}(r,\varphi) = (\mathbf{e}_x + i\mathbf{e}_y) e^{im\varphi} F_{m,N}(r), \\
 \mathbf{e}_{-,m,N}^- &= \mathbf{e}_{m,N}^{(1)}(r,\varphi) - i\mathbf{e}_{m,N}^{(3)}(r,\varphi) = (\mathbf{e}_x - i\mathbf{e}_y) e^{-im\varphi} F_{m,N}(r), \\
 \mathbf{e}_{+,m,N}^- &= \mathbf{e}_{m,N}^{(2)}(r,\varphi) + i\mathbf{e}_{m,N}^{(4)}(r,\varphi) = (\mathbf{e}_x - i\mathbf{e}_y) e^{im\varphi} F_{m,N}(r), \\
 \mathbf{e}_{-,m,N}^+ &= \mathbf{e}_{m,N}^{(2)}(r,\varphi) - i\mathbf{e}_{m,N}^{(4)}(r,\varphi) = (\mathbf{e}_x + i\mathbf{e}_y) e^{-im\varphi} F_{m,N}(r).
 \end{aligned} \tag{14}$$

Thus, if polarized radiation with the right or left circular polarization is incident on the input of the fiber, the modes with $m = 0$ and $m > 1$ will retain the state of polarization.

Polarized light with arbitrary state of polarization of light can be presented as superposition of light with the left and right circular polarization. Let us use Jones calculus (Azzam & Bashara, 1977; Gerrard & Burch, 1975) to describe the propagation of polarized quasi-monochromatic plane light wave along z -axis. Normalized Jones vector of the wave with arbitrary state of polarization can be presented in the following reductive form:

$$\mathbf{E} = \begin{pmatrix} A \\ B \cdot e^{i\delta} \end{pmatrix}, \tag{15}$$

here $A = |E_x|/|\mathbf{E}|$, $B = |E_y|/|\mathbf{E}|$, $|\mathbf{E}| = \sqrt{|E_x|^2 + |E_y|^2}$ and $\delta = \delta_x - \delta_y$. Arbitrary Jones vector can be represented as a linear combination:

$$\mathbf{E} = C_L \cdot \frac{1}{\sqrt{2}} \begin{pmatrix} 1 \\ -i \end{pmatrix} + C_R \cdot \frac{1}{\sqrt{2}} \begin{pmatrix} 1 \\ +i \end{pmatrix} \tag{16}$$

The coefficients C_L and C_R determine the contribution of left-handed and right-handed circular polarized light into the state of polarization defined by Jones vector \mathbf{E} . The coefficients depend on the angle of ellipticity ε , and the angle ε depends on ellipticity e in the following way:

$$e = \operatorname{tg} \varepsilon, \quad e = \frac{b}{a}, \quad (17)$$

where a is the length of a large semi axis of polarization ellipse and b is the length of a small semi axis of polarization ellipse. Following (Azzam & Bashara, 1977) represent the coefficients C_L and C_R as a function of the angle of ellipticity ε :

$$\begin{aligned} C_L &= \frac{1}{\sqrt{2}}(\cos \varepsilon - \sin \varepsilon), \\ C_R &= \frac{1}{\sqrt{2}}(\cos \varepsilon + \sin \varepsilon). \end{aligned} \quad (18)$$

Let $\mathbf{E}_0(r, \varphi)$ is the field of light wave falling on the input end of an optical fiber with the length z . The arbitrary state of polarization of the wave is defined by a normalized Jones vector Eq. (15). Then

$$\mathbf{E}_0(r, \varphi) = C_L \frac{1}{\sqrt{2}} \begin{pmatrix} 1 \\ -i \end{pmatrix} \cdot E_0^-(r, \varphi) + C_R \frac{1}{\sqrt{2}} \begin{pmatrix} 1 \\ +i \end{pmatrix} \cdot E_0^+(r, \varphi), \quad (19)$$

where $E_0^-(r, \varphi)$ is the amplitude of light wave with left-handed circular state of polarization at the optical fiber input, $E_0^+(r, \varphi)$ is the amplitude of light wave with right-handed circular state of polarization at the optical fiber input. To describe the propagation of linearly polarized light or light with the arbitrary state of polarization through the fiber, it is possible to consider propagation through the fiber of light with circular polarization at the fiber input. According to the results of the paper (Darsht et al., 1995):

$$\begin{aligned} E_0^+ &= A_{\text{right}}(r, \varphi, z = 0) = e^{-i\varphi} \sum_N B_{1,N} F_{1,N}(r) + \sum_{m \neq 1} \sum_N B_{m,N} e^{-im\varphi} F_{m,N}(r) \\ &\quad + \sum_m \sum_N A_{m,N} e^{im\varphi} F_{m,N}(r), \end{aligned} \quad (20)$$

$$\begin{aligned} E_0^- &= A_{\text{left}}(r, \varphi, z = 0) = e^{i\varphi} \sum_N A_{1,N} F_{1,N}(r) + \sum_{m \neq 1} \sum_N A_{m,N} e^{im\varphi} F_{m,N}(r) \\ &\quad + \sum_m \sum_N B_{m,N} e^{-im\varphi} F_{m,N}(r). \end{aligned} \quad (21)$$

Here those modes which do not retain circular polarization under propagation through the fiber are selected. It is necessary to underline that in case of the linear polarization at the fiber input the modes $\mathbf{e}_{+,m,N}^+(r, \varphi)$ and $\mathbf{e}_{+,m,N}^-(r, \varphi)$ give equal contribution to the propagating light, and this contribution is determined by the coefficient $A_{m,N}$. The modes $\mathbf{e}_{-,m,N}^+(r, \varphi)$ and $\mathbf{e}_{-,m,N}^-(r, \varphi)$ give the equal contribution to the propagating light as well, and this contribution is determined by the coefficient $B_{m,N}$. Values of coefficients $A_{m,N}$ and $B_{m,N}$ determine the intensity distribution at the fiber input. They are selected by means of a random-number generator in our investigation, but the optimum condition of the effect observation can depend on their relative value. Following the results of the paper Darsht et al. (1995) we have the following distribution of the amplitude of the light field $\mathbf{E}^-(r, \varphi, z)$ and $\mathbf{E}^+(r, \varphi, z)$ at

the fiber output:

$$\begin{aligned}
 \mathbf{E}^+(r, \varphi, z) &= \mathbf{E}^{++}(r, \varphi, z) + \mathbf{E}^{+-}(r, \varphi, z) = \\
 &= \frac{1}{\sqrt{2}} \begin{pmatrix} 1 \\ i \end{pmatrix} \cdot \left\{ \sum_{m \neq 1} \sum_N B_{m,N} e^{-im\varphi} F_{m,N}(r) e^{iz(\beta_{m,N} + \delta\beta_{m,N}^{(2)})} \right. \\
 &\quad + \sum_m \sum_N A_{m,N} e^{+im\varphi} F_{m,N}(r) e^{iz(\beta_{m,N} + \delta\beta_{m,N}^{(1)})} \\
 &\quad \left. + \sum_N B_{1,N} e^{-i\varphi} F_{1,N}(r) e^{iz\beta_{1,N}} \left(e^{i2z\delta\beta_{1,N}^{(2)}} + 1 \right) \right\} \\
 &+ \frac{1}{\sqrt{2}} \begin{pmatrix} 1 \\ -i \end{pmatrix} \cdot \left[e^{+i\varphi} \sum_N B_{1,N} F_{1,N}(r) e^{iz\beta_{1,N}} \left(e^{i2z\delta\beta_{1,N}^{(2)}} - 1 \right) \right]. \quad (22)
 \end{aligned}$$

$$\begin{aligned}
 \mathbf{E}^-(r, \varphi, z) &= \mathbf{E}^{--}(r, \varphi, z) + \mathbf{E}^{-+}(r, \varphi, z) = \\
 &= \frac{1}{\sqrt{2}} \begin{pmatrix} 1 \\ -i \end{pmatrix} \cdot \left\{ \sum_{m \neq 1} \sum_N A_{m,N} e^{+im\varphi} F_{m,N}(r) e^{iz(\beta_{m,N} + \delta\beta_{m,N}^{(2)})} \right. \\
 &\quad + \sum_m \sum_N B_{m,N} e^{-im\varphi} F_{m,N}(r) e^{iz(\beta_{m,N} + \delta\beta_{m,N}^{(1)})} \\
 &\quad \left. + \sum_N A_{1,N} e^{+i\varphi} F_{1,N}(r) e^{iz\beta_{1,N}} \left(e^{i2z\delta\beta_{1,N}^{(2)}} + 1 \right) \right\} \\
 &+ \frac{1}{\sqrt{2}} \begin{pmatrix} 1 \\ i \end{pmatrix} \cdot \left[e^{-i\varphi} \sum_N A_{1,N} F_{1,N}(r) e^{iz\beta_{1,N}} \left(e^{i2z\delta\beta_{1,N}^{(2)}} - 1 \right) \right]. \quad (23)
 \end{aligned}$$

The intensity of the light at the optical fiber output $I^+(r, \varphi, z)$ and $I^-(r, \varphi, z)$ are the following:

$$I^+(r, \varphi, z) = \mathbf{E}^+(r, \varphi, z) \cdot (\mathbf{E}^+)^*(r, \varphi, z) = |C_R(z)|^2 \cdot |\mathbf{E}^{++}(r, \varphi, z)|^2 + |C_L(z)|^2 \cdot |\mathbf{E}^{+-}(r, \varphi, z)|^2.$$

$$I^-(r, \varphi, z) = \mathbf{E}^-(r, \varphi, z) \cdot (\mathbf{E}^-)^*(r, \varphi, z) = |C_R(z)|^2 \cdot |\mathbf{E}^{-+}(r, \varphi, z)|^2 + |C_L(z)|^2 \cdot |\mathbf{E}^{--}(r, \varphi, z)|^2.$$

One can see from Eqs. (22) and (23) that circular polarization does not conserve under the light propagation through an optical fiber with step index profile. All described above is used in the following sections.

3. Theoretical prediction and the experimental investigation of the isolated wave front dislocation formation

Here the possibility of the formation of a wavefront with an isolated screw dislocation of a given sign during the propagation of circularly polarized light through a multimode optical fiber is described. It follows from Eq.(22) and Eq. (23), that only the modes $\mathbf{e}_{1,N}^2$ and $\mathbf{e}_{1,N}^4$ contribute to the "foreign" polarization under circularly polarized light propagation through a multimode fiber. In the geometrical optics interpretation the modes $\mathbf{e}_{1,N}^2$ and $\mathbf{e}_{1,N}^4$ correspond to meridional rays for which circular polarization is not conserved because of symmetry consideration (Baranova & Zel'dovich, 1994; Snyder & Love, 1984). If a "circular analyzer"

transmitting circular radiation opposite in sign to σ at the fiber input is placed at the fiber exit, only the corresponding modes with $m = 1$ will be transmitted through that analyzer. Let us consider the field passing through the "circular analyzer" in greater detail. This field is described by the last term in Eq. (22) and Eq. (23). If light with $\sigma = 1$ enters the fiber the field with $\sigma = -1$ transmitted through the "circular analyzer" will have the following form:

$$\mathbf{E}^{+-} = \exp(i\varphi) \cdot \frac{1}{\sqrt{2}} \begin{pmatrix} 1 \\ -i \end{pmatrix} \cdot \left\{ \sum_N B_{1,N} F_{1,N}(r) \exp(iz\beta_{1,N}) \left[\exp\left(i2z\delta\beta_{1,N}^{(2)}\right) - 1 \right] \right\}. \quad (24)$$

The factor $\exp(i\varphi)$ indicates that the wavefront of the field (Eq. 24) contains one positive screw dislocation. If the entrance of the waveguide is illuminated with circularly polarized radiation with $\sigma = -1$ and circularly polarized radiation with $\sigma = +1$ is extracted at the fiber exit, the field E^{-+} after the "circular analyzer" will have the following form:

$$\mathbf{E}^{-+} = \exp(-i\varphi) \cdot \frac{1}{\sqrt{2}} \begin{pmatrix} 1 \\ +i \end{pmatrix} \cdot \left\{ \sum_N A_{1,N} F_{1,N}(r) \exp(iz\beta_{1,N}) \left[\exp\left(i2z\delta\beta_{1,N}^{(2)}\right) - 1 \right] \right\}. \quad (25)$$

It means that the light field (Eq. 25) contains one negative screw dislocation.

It follows from Eq. (24) and Eq. (25) that the intensity distribution $I^{+-} = E^{+-} \cdot (E^{+-})^*$ across the fiber does not depend on the angle φ , i.e., the intensity distribution has axial symmetry. In the special case of an optical fiber with a small number of modes, such as $N_{\max} = 1$ for $m = 1$, the intensity of the "foreign" polarization is a periodic function of the fiber length:

$$I^{+-} = (B_{1,1} F_{1,1}(r))^2 \left[1 - \cos(2z\delta\beta_{1,1}^{(2)}) \right]. \quad (26)$$

$$I^{-+} = (A_{1,1} F_{1,1}(r))^2 \left[1 - \cos(2z\delta\beta_{1,1}^{(2)}) \right]. \quad (27)$$

The intensity I^{+-} and I^{-+} are maximum for fiber lengths

$$z_n = \frac{\pi(2n-1)}{2\delta\beta_{1,1}^{(2)}}. \quad (28)$$

The intensity I^{+-} and I^{-+} are minimum for fiber lengths

$$z_n = \frac{n\pi}{\delta\beta_{1,1}^{(2)}}. \quad (29)$$

Therefore, if circularly polarized radiation with a definite sign of σ is injected into a multimode fiber with a step like index profile and circularly polarized radiation of the opposite sign σ is extracted at the fiber exit, the transmitted radiation will consist of a light wave with an isolated wavefront dislocation, and a sign change of σ at the fiber input together with a corresponding sign change of the "circular analyzer" will result in the change of the screw dislocation sign.

Figure 1a shows the calculated intensity distribution of the interference pattern in the case of a plane wave and a converging wave $\mathbf{E} \sim \mathbf{A}(\mathbf{r}, z, t)e^{i\varphi}$ with a positive dislocation, and Fig. 1b shows calculated intensity distribution of the interference pattern in the case of a plane wave and a converging wave with a negative dislocation. As one can see in Fig. 1, the interference pattern is a spiral which unwinds in the clockwise direction in the case of a

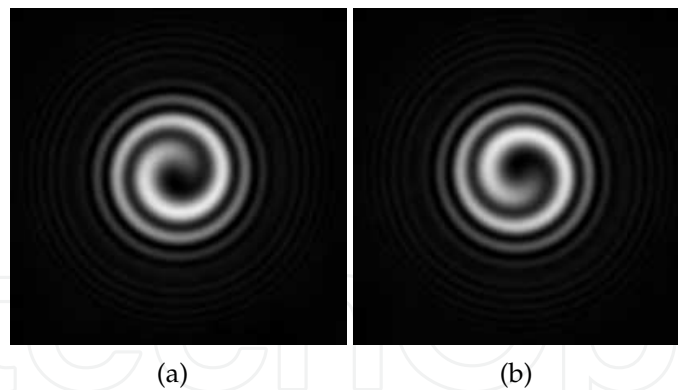


Fig. 1. Interference patterns in the case of a plane wave and a converging wave with a positive dislocation (a) and calculated intensity distribution of the interference pattern in the case of a plane wave and a converging wave with a negative dislocation (b).

single positive screw dislocation and in the counterclockwise direction in the case of a single negative screw dislocation. It follows from Fig. 1 that the change of the screw dislocation sign results in the change of the spiral direction unwinding. That means, that when the sign of the circular polarization at the fiber input and output changes, the direction of the spiral unwinding should also change.

The experimental generation of a light wave with a wavefront dislocation has been done using an optical fiber with a step like index profile and the following parameters: fiber core diameter $2\rho = 9 \mu\text{m}$, difference between the refractive index of the core and cladding $\delta n = n_{\text{co}} - n_{\text{cl}} = 0.004$. According to Eq. (8) twelve modes can propagate through the fiber:

$$\begin{aligned} M_1 &= \mathbf{e}_{0,1}^{(1)}(r, \varphi) & M_2 &= \mathbf{e}_{0,1}^{(3)}(r, \varphi) & M_3 &= \mathbf{e}_{0,2}^{(1)}(r, \varphi) & M_4 &= \mathbf{e}_{0,2}^{(3)}(r, \varphi) \\ M_5 &= \mathbf{e}_{1,1}^{(1)}(r, \varphi) & M_6 &= \mathbf{e}_{1,1}^{(2)}(r, \varphi) & M_7 &= \mathbf{e}_{1,1}^{(3)}(r, \varphi) & M_8 &= \mathbf{e}_{1,1}^{(4)}(r, \varphi) \\ M_9 &= \mathbf{e}_{2,1}^{(1)}(r, \varphi) & M_{10} &= \mathbf{e}_{2,1}^{(2)}(r, \varphi) & M_{11} &= \mathbf{e}_{2,1}^{(3)}(r, \varphi) & M_{12} &= \mathbf{e}_{2,1}^{(4)}(r, \varphi). \end{aligned} \quad (30)$$

The optimum fiber length has been calculated and determined in accordance with Eq.(28). The polarization correction $\delta\beta_{1,1}^{(2)}$ has been found to be 0.20526^{-1} . As it was stated above the part of "foreign" polarization in intensity of light at the end of a fiber is periodical, that can also be seen in Fig. 2 for a fiber with parameters described above. The length of the fiber under investigation $z = 114 \text{ cm}$ corresponded to $n = 7$ in Eq. (28). A Mach-Zender interferometer scheme was used to record the wavefront with an isolated dislocation. It should be stressed that an adjustable polarization system with the quarter wave property (Goltser et al., 1993) has been used for "circular polarizer" and "circular analyzer". The device provided up to 98% circular polarization.

Figure 3 shows photos of the interference pattern of a plane wave and the converging wave under investigation. Figure 3a illustrates the situation when circularly polarized light with $\sigma = +1$ is incident upon the fiber input and a circularly polarized light wave with $\sigma = -1$, containing a positive screw wavefront dislocation, is extracted by the "circular analyzer." As one can see in Fig. 3a, the interference pattern is a clockwise spiral. Comparing with Fig. 1a shows that this result agrees completely with theory. Figure 3b displays a photo of the interference pattern of a plane wave and the wave under investigation with a negative wavefront dislocation. The interference pattern unwinds in the counterclockwise direction

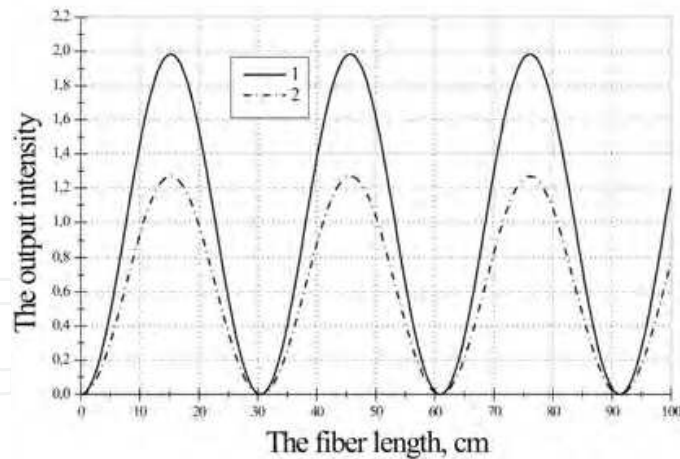


Fig. 2. The dependence of "foreign" polarization part in the output intensity of light on the fiber length at the illumination the fiber with right hand (1) and left hand (2) circularly polarized light.

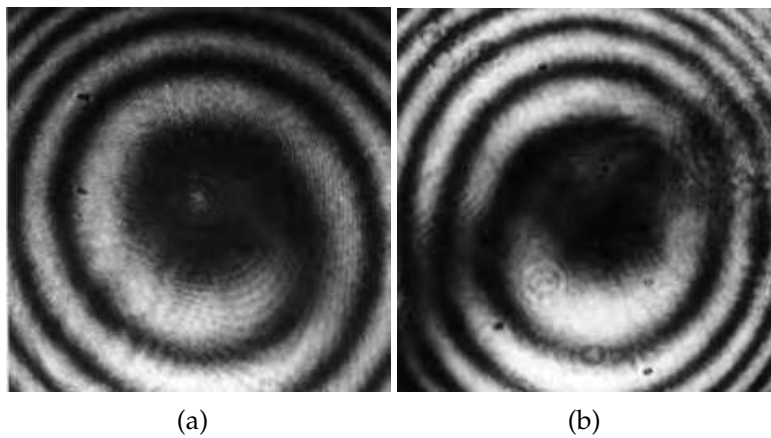


Fig. 3. Photos of the interference pattern on the screen. a - Circularly polarized radiation with $\sigma = +1$ is incident at fiber input and circularly polarized radiation with $\sigma = -1$ is extracted from the output radiation. b - Circularly polarized radiation with $\sigma = -1$ is incident at fiber input and circularly polarized radiation with $\sigma = +1$ is extracted from the output radiation.

like the spiral in Fig. 1b. Therefore, this result also agrees completely with the expected result. It should be emphasized that only one spiral is observed in the interference pattern in Figs. 3a and 3b; this corresponds to an isolated wavefront dislocation.

As a result of this work, the possibility of the formation of a light wave with an isolated wavefront dislocation having a fixed sign has been proved. Such a wave is formed when polarized radiation passes through a multimode optical fiber placed between crossed "circular polarizers". The sign of the dislocation changes when the sign of the "circular polarizers" at the fiber input and exit changes.

4. The optical Magnus effect and its peculiarity in a few modes fiber

As it has been mentioned above, optical Magnus effect manifests itself as speckle pattern rotation of circular polarized light transmitted through a multimode step-index fiber under

circular polarization sign change (Doogin et al., 1992; 1991). Using Eq. (22) and Eq. (23) let us consider a case when we illuminate a multimode optical fiber by right and left polarization in turn, but with strictly the same modal distribution at the input and omit all modes with $m = 1$. Eq. (22) and Eq. (23) take the following form.

$$\mathbf{E}^+(r, \varphi, z) = \frac{1}{\sqrt{2}} \begin{pmatrix} 1 \\ i \end{pmatrix} \cdot \left\{ \sum_{m \neq 1} \sum_N C_{-,m,N} e^{-im\varphi} F_{m,N}(r) e^{iz(\beta_{m,N} + \delta\beta_{m,N}^{(2)})} + \sum_m \sum_N C_{+,m,N} e^{+im\varphi} F_{m,N}(r) e^{iz(\beta_{m,N} + \delta\beta_{m,N}^{(1)})} \right\} \quad (31)$$

$$\mathbf{E}^-(r, \varphi, z) = \frac{1}{\sqrt{2}} \begin{pmatrix} 1 \\ -i \end{pmatrix} \cdot \left\{ \sum_{m \neq 1} \sum_N C_{+,m,N} e^{+im\varphi} F_{m,N}(r) e^{iz(\beta_{m,N} + \delta\beta_{m,N}^{(2)})} + \sum_m \sum_N C_{-,m,N} e^{-im\varphi} F_{m,N}(r) e^{iz(\beta_{m,N} + \delta\beta_{m,N}^{(1)})} \right\} \quad (32)$$

Let us compare the angular intensity distributions for the left handed ($\sigma = -1$) and right handed ($\sigma = +1$) circular polarizations in some cross-section. Fig. 4 shows the

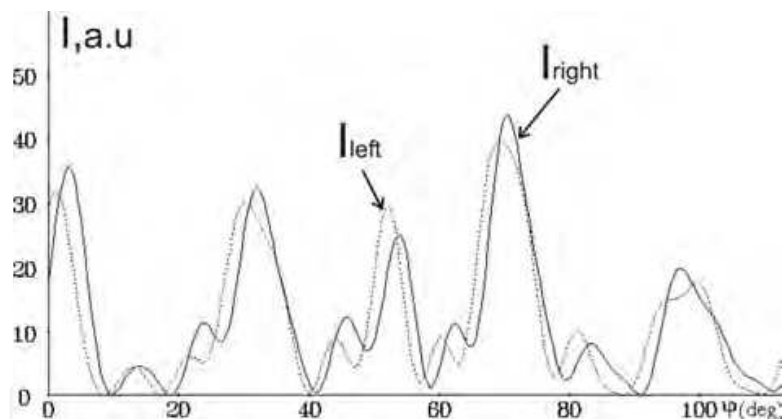


Fig. 4. The angular intensity distributions for the left handed ($\sigma = -1$) and right handed ($\sigma = +1$) circular polarizations in some fiber cross-section

speckle-patterns particular realization for the left and right circular polarizations. It can be seen from Fig. 4 that the whole picture suffers angular shift (rotation) saving main features and being slightly distorted under the change of the circular polarization. To extract the pure rotation from the whole change of the speckle-pattern the correlation function has been calculated.

The first experimental observation of the speckle pattern rotation under the change of the circular polarization has been done using a fiber with the following parameters. The fiber diameter was $2\rho = 200 \mu\text{m}$; the difference between refractive indices of quartz core and polymeric cladding $\Delta n = n_{\text{co}} - n_{\text{cl}} = 0.006$ was measured via the critical angle of propagating rays; the fiber length was 96 cm.

Changing circular polarization of propagating light from left-handed to right-handed resulted in the speckle pattern flowing clock-wise in accordance with the theoretical prediction. During that flowing some details of speckle-pattern changed, but the main features were conserved under rotation. The fragments of the speckle-patterns for both circular polarizations are shown in Fig. 5. The arrow points out the bright sport that was rotated slightly changing

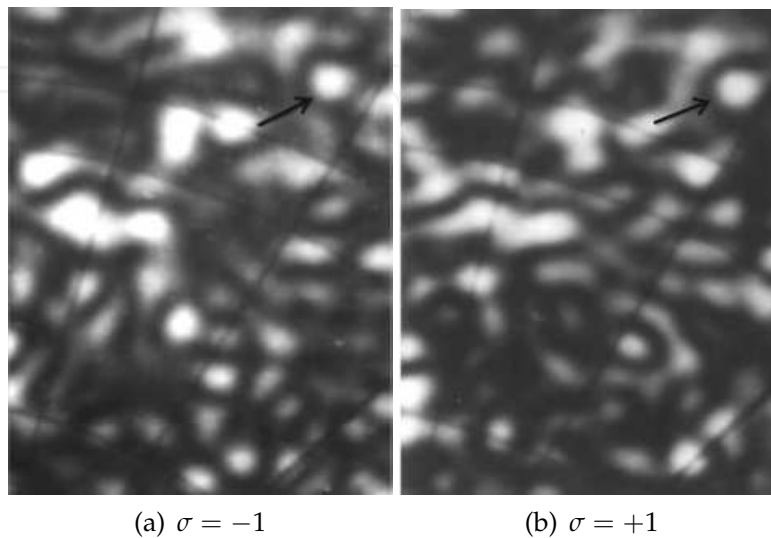


Fig. 5. The fragment of the real speckle-patterns of right-hand ($\sigma = +1$) and left-hand ($\sigma = -1$) circularly polarized light at the screen. The arrow points out the bright spot as an example of rotation under circular polarization sign change

its shape (just like it was in the computer experiment, see Fig.4).

In order to determine the "rotation angle" an experimental analog of the correlation function technique was used in the paper (Doogin et al., 1992). The negative slide for the right-handed circular polarization speckle-pattern was projected to the positive photograph of the left-handed one and the least contrast was achieved by their mutual rotation. The angle between the two coordinate nets corresponding to the contrast minimum was regarded as the "rotation angle". It was $(1.4 \pm 0.5)^\circ$ for the fiber under investigation.

For the first time optical Magnus effect has been observed in a multi-mode optical fiber (Doogin et al., 1992; 1991), and all calculations of the speckle pattern rotation angle have also been done (Doogin et al., 1992) for a multimode fiber, but the influence of meridional rays has been neglected. Using the wave interpretation we can associate meridional rays with TE and TM modes. Their combination is circular polarized, but due to the difference of their propagation velocity circular polarization does not keep unchanged in contrast to all other skew rays. In the case of multimode fiber contribution of meridional rays can be neglected but the speckle pattern rotation angle in such fibers is too small, of order 0.1 degree per 1 centimeter of fiber's length. In a few mode fibers rotation angle is two orders larger, but the contribution of meridional rays is noticeable.

One can see from Eq. 22 and Eq. (23) that during propagation of light with "original" polarization "foreign" polarization appears due to the presence of modes with $m = 1$ (TE and TM modes). The contribution of these modes has a periodical nature along the fiber length.

To calculate the light intensity distribution across the fiber cross section Eq. 22 and Eq. (23) were used. In Fig. 6 speckle patterns at the end of the fiber with following parameters: $2\rho = 9 \mu\text{m}$

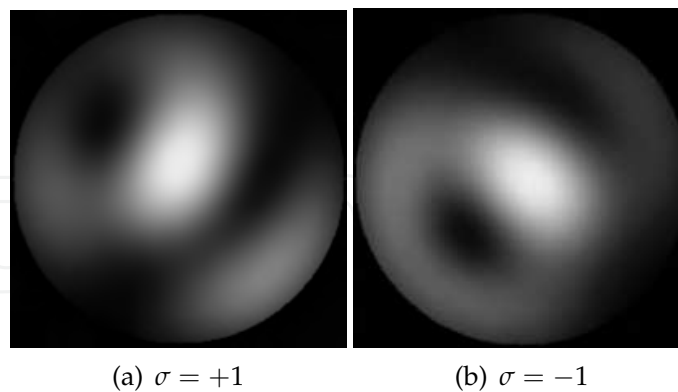


Fig. 6. Speckle patterns at the end of the fiber with following parameters: $2\rho = 9 \mu\text{m}$, $n_{\text{co}} = 1.47$, $\delta n = 0.004$, $z = 18 \text{ cm}$, $\lambda = 0.6328 \mu\text{m}$.

μm , $n_{\text{co}} = 1.47$, $\delta n = 0.004$, $z = 18 \text{ cm}$, $\lambda = 0.6328 \mu\text{m}$ are presented. It can be seen in Fig. 6 that this fiber is a few mode fiber. A rotation of speckle patterns can be observed. The number of maximal remains the same, but their intensities change due to modes with $m = 1$.

Regardless the modes with $m = 1$, the rotation with no change of maximal intensity will be observed. It is well known that the number of modes propagating in optical fiber depends on the radius of the fiber's core, the difference between refractive indices of the core and the cladding and the wavelength. To determine the fiber parameters for which the contribution of modes with $m = 1$ becomes noticeable the speckle pattern rotation angles for different diameters of fiber core (Fig. 7) were calculated. The calculation was realized in two ways:

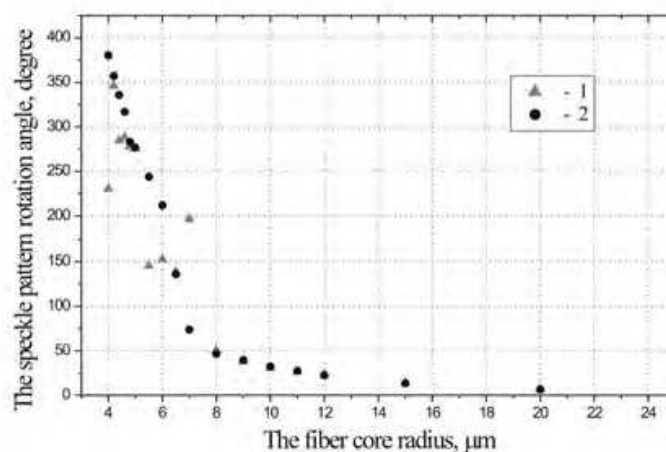


Fig. 7. The dependence of speckle pattern rotation angle on the fiber core radius: taking modes with $m = 1$ into consideration (1) and neglecting those modes (2).

taking modes with $m = 1$ into consideration and neglecting those modes. Figure 7 indicates that at $\rho \geq 8 \mu\text{m}$ we can neglect the contribution of modes with $m = 1$ and the rotation angle is $\sim 50^\circ$ at length 18 cm.

As it can be seen in Fig. 2 the contribution of modes with $m = 1$ is equal to 0 at length multiple to ~ 30 cm. We should suppose that for this fiber the rotation of speckle pattern can take place only at this length. At the length multiple to ~ 15 cm it will be no rotation due to maximal contribution of modes with $m = 1$. In order to examine this supposition the dependence of speckle pattern rotation on fiber length was computed (Fig. 8). The software calculating the

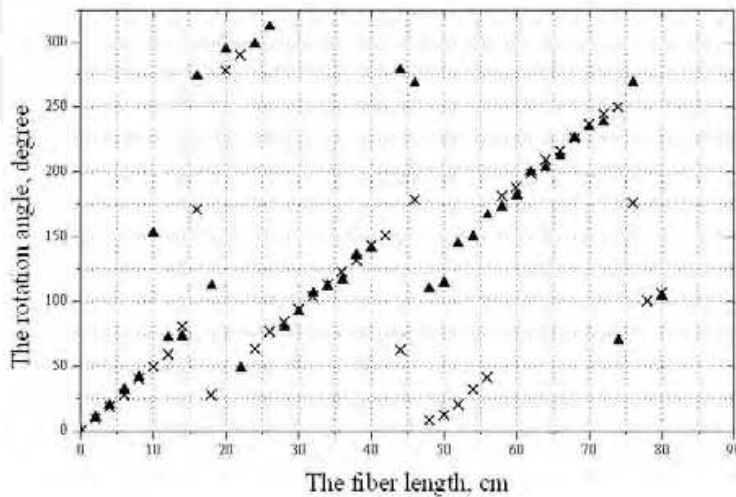


Fig. 8. The speckle pattern rotation angle dependence on the fiber length for two different realization of speckle pattern

rotation angle between two speckle patterns yields the value of rotation angle even if there is no rotation. In this case the obtained value differs from the expected one immensely. This is a cause of the scattering of points in Fig. 8. At the length multiple to ~ 15 cm the scattering is maximal (rotation is absent). At the length multiple to ~ 30 cm there is almost no scattering. In this case the rotation can be observed visually on the computer screen that confirms our supposition. Thus, the optimal length for optical Magnus effect observation in the fiber with present parameters is multiple to ~ 30 cm.

Experimental investigations were carried out at a fiber with step like index profile and $2\rho = 9 \mu\text{m}$, $n_{\text{co}} = 1.47$, the numerical aperture $N_A = 0.11$ at the wavelength $\lambda = 0.6326 \mu\text{m}$. Optical Magnus effect was distinctly observed at the small fiber length in the range from 4 till 20 cm. The experimental results are presented in Fig.9. The calculated dependence of the speckle pattern rotation angle on the fiber length is shown in Fig. 9 too. One can see in Fig. 9 that the angle of the speckle pattern rotation depends on the fiber length linearly, but there is difference in the slope of the experimental and theoretical lines. It can be connected with the speckle pattern distortion.

The influence of the meridional modes contribution on the optical Magnus effect in fibers with different numbers of modes has been demonstrated.

5. The influence of light polarization on the speckle pattern of the polarized light transmitted through multimode optical fiber

Let us consider the propagation of arbitrary polarized light through an axially symmetric optical fiber with a step like refractive index profile. The arbitrary state of polarization

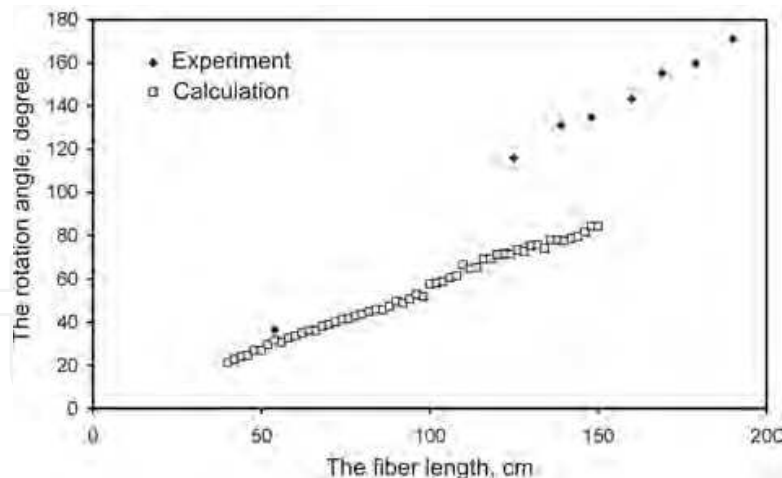


Fig. 9. Experimental and calculated the speckle pattern rotation angle as a function of the fiber length for the fiber with the diameter $2\rho = 9 \mu\text{m}$, the core refractive index $n_{\text{co}} = 1.47$, numerical aperture $N_A = 0.11$ at the wavelength $\lambda = 0.6328 \mu\text{m}$.

is defined by the ellipticity angle ε . The contribution of the intensity of the right circular polarized light to the whole intensity β_r is defined by the following way:

$$\beta_r = |C_R|^2 = \frac{1}{2}(\cos \varepsilon + \sin \varepsilon)^2. \quad (33)$$

Here the coefficient C_R is defined by Eq.18. In order to determine the light intensity distribution across the fiber section at the fiber output end (speckle pattern) $I(r, \varphi, z)$ as a function of β_r at the fiber input Eq. (24) has been used.

A multimode optical fiber with a step like index profile and $\rho = 50 \mu\text{m}$, $n_{\text{co}} = 1.47$, $n_{\text{cl}} = 1.454$, $n_{\text{co}} - n_{\text{cl}} = \Delta n = 0.016$ has been chosen for experimental investigation. Optical Magnus effect is distinctly observed in this fiber. Calculation of the speckle patterns according to Eq. (24) has been carried out for a fiber with the same parameters. Figure 10 shows the dependence of the speckle pattern angle rotation ψ on the fiber length z for two various mode structure (different sets of coefficients $A_{m,N}$ and $B_{m,N}$) of light propagating through the optical fiber under investigation. One can see in Fig. 10, that there is some critical length $z_{\text{max}} \approx 15$. If the fiber length is less than critical length z_{max} , the dependence $\psi(z)$ will be linear and the rotation angle will increase with the increase of the fiber length. If the fiber length is greater than critical length z_{max} the rotation angle will decrease with the increase of the fiber length. This behavior can be explained by the relative angular size of the single speckle φ_{speckle} . The speckle pattern rotation will be distinctly observed only if $\psi < \varphi_{\text{speckle}}$.

Two pieces of the fiber of different length have been chosen for experimental investigation. The length of the first fiber was almost critical ($z = 15.4 \text{ cm}$) and the length of the second fiber was greater than the critical length ($z = 20.5 \text{ cm}$). Radiation of He-Ne laser with wave length $\lambda = 0.628 \mu\text{m}$ has been used under experimental investigation. The polarizing system consisting of a polarizer and an adjustable quarter wave plate (Goltser et al., 1993) allowed to change the light polarization state from right circular polarization $\beta_r = 1$ to left circular polarization $\beta_r = 0$. Value $\beta_r = 0.5$ corresponds to linear polarized light. The images of speckle patterns of light at the fiber exit have been registered in a digital form. The special software was used for the speckle patterns analysis of the determination and for the rotation angle.

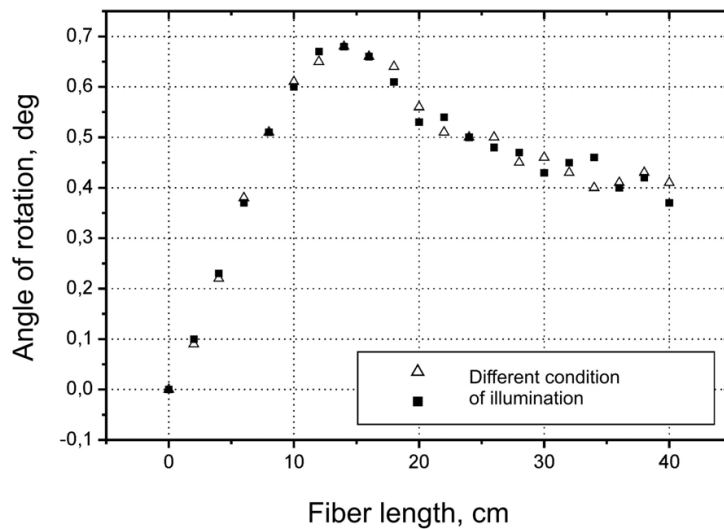


Fig. 10. Dependence of the speckle pattern angle rotation on the fiber length for two various mode structure of light propagating through the optical fiber under investigation.

Figure 11 shows speckle patterns of the light at the output end of the fibers with the length

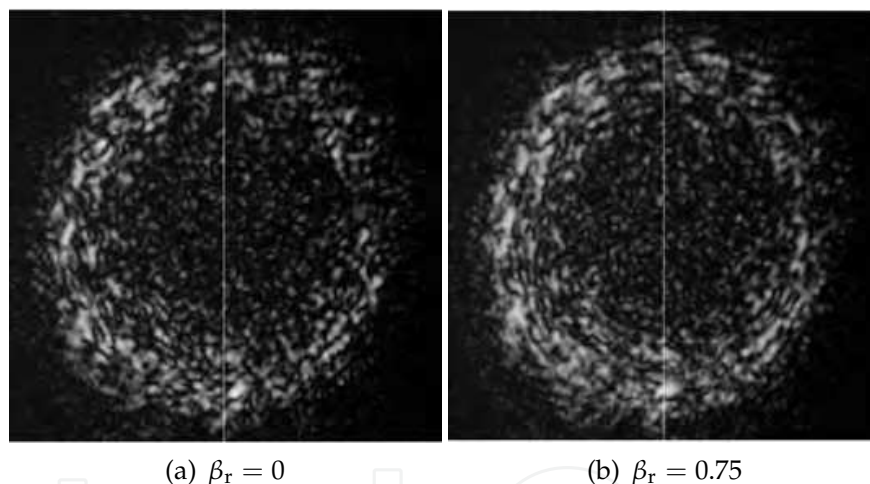


Fig. 11. Images of speckle patterns of radiation with the left circular polarization (a) and elliptic polarization (b) at the fiber output. The fiber length is $z = 15.4$ cm.

$z = 15.4$ cm. Image in Fig. 11a corresponds to the left circular polarization at the fiber input ($\beta_r = 0$), image in Fig. 11b corresponds to the elliptical polarization at the fiber input with $\beta_r = 0.75$. Radiation was entered into the fiber under some angle to the fiber axis, as a result the speckle pattern had the form of a ring (Zel'dovich et al., 1996). It can be seen in Fig. 11, that the main speckle pattern features are kept unchanged under the change of the relative contribution of the right circular polarized light, the speckle rotation was distinctly observed visually. The speckle pattern rotation was also confirmed by the computer processing of the images, the angle of rotation was determined. The speckle pattern rotation was also observed under other states of polarization change. Figure 12 and Fig. 13 show the experimental and calculated angles of the speckle pattern rotation ψ as a function of the contribution of light with the right circular polarization β_r into the elliptical polarization for the fiber length $z =$

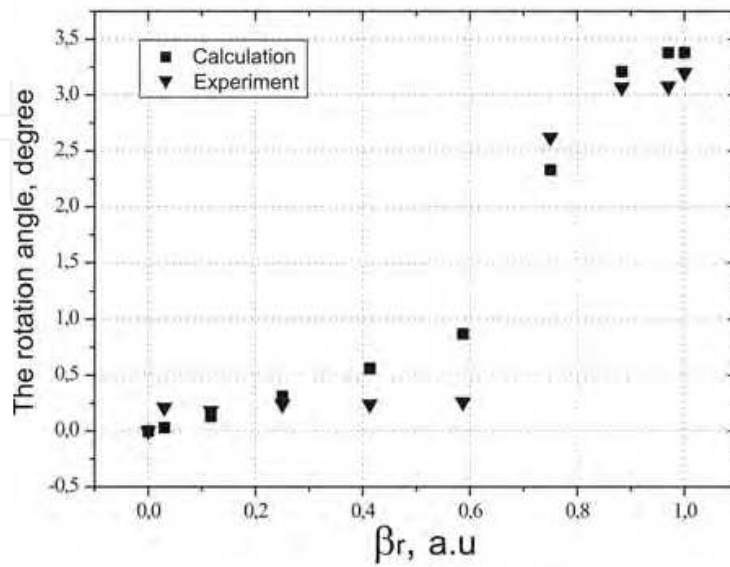


Fig. 12. The experimental and calculated angles of the speckle pattern rotation ψ as a function of the contribution of light with the right circular polarization β_r into the elliptical polarization for the fiber length $z = 20.5$ cm.

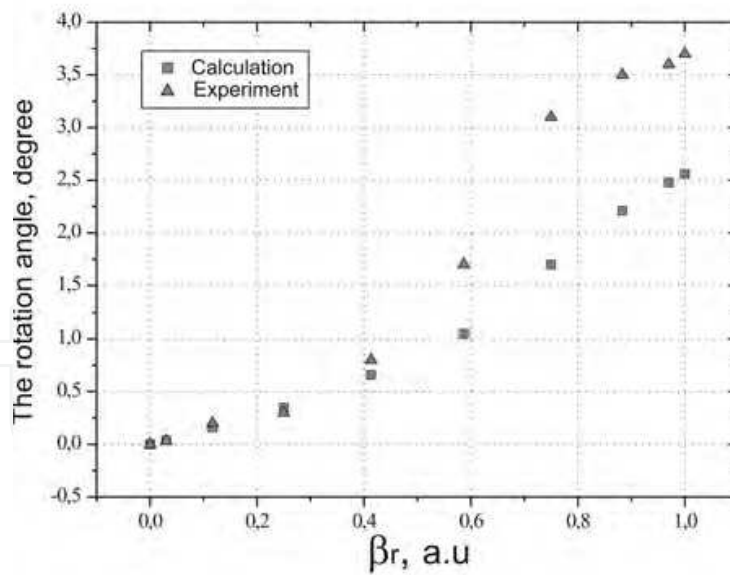


Fig. 13. The experimental and calculated angles of the speckle pattern rotation ψ as a function of the contribution of light with the right circular polarization β_r into the elliptical polarization for the fiber length $z = 15.4$ cm.

15.4 cm and $z = 20.5$ cm. Figure 12 and Fig. 13 demonstrate qualitative and quantitative coincidence of the experimental results and the results of calculation.

To sum up, the change of the light ellipticity at the optical fiber input results in speckle pattern rotation at the fiber output and the angle of rotation depends linearly on the contribution of the light intensity with right-handed circular polarization into the intensity with the elliptical state of polarization. The length of the fiber where the linear dependence of ψ (β_r) is observed is determined by optical fiber parameters.

6. The influence of external magnetic field on the speckle pattern behavior

It is well known that under light propagation through an optical medium placed in an external magnetic field a rotation of the polarization plane of linearly polarized light is observed. This rotation is a result of the changes of the refractive indexes of light with the left and right circular polarization under the influence of a magnetic field. However no marked change of the trajectory of light was observed. It has been shown by (Baranova & Zel'dovich, 1994), that the influence of a magnetic field on light propagation in an optical fiber located in a longitudinal magnetic field can result in noticeable rotation of a speckle pattern and the angle of rotation φ will be proportional to the Verdet constant V , value of the magnetic field H and the length of the fiber in the magnetic field z :

$$\varphi \approx VHz.$$

For the observation of this effect it was proposed to illuminate the input of a fiber with linearly polarized light, and to choose the linearly polarized component with the same azimuth in light passed through a fiber. In the paper (Baranova & Zel'dovich, 1994) theoretical analysis of the effect was carried out within the framework of the elementary model in which light propagation in an axial symmetric optical fiber which keeps in scalar approach only three modes was considered.

The experimental results obtained in the paper (Darsht et al., 1994) have shown that such a rotation can really be observed, and the direction of the rotation varies on the change of the external magnetic field direction. The effect of the magnetic rotation of the speckle pattern was observed under light propagation through a quartz fiber. The value of the Verdet constant for quartz at the wavelength $\lambda = 0.633 \mu\text{m}$ is equal to $V = 1.4 \cdot 10^{-2} \text{ min}/(\text{Gs} \cdot \text{cm})$ that can provide the rotation of the speckle pattern over the angle $\theta \approx 2^\circ$ at the value of the magnetic field $H = 500 \text{ Gs}$ and the length of the fiber in the magnetic field 21.5 cm. To enhance the effect (Darsht et al., 1994) the fiber was passed through a solenoid with a magnetic field some times, so that the length of the fiber in the magnetic field increased up to 140 cm. The angle of the rotation of the speckle pattern was determined at the change of the direction of the magnetic field $H = 500 \text{ Gs}$ and it was equal to 15° . The angle of the Faraday rotation would be $\approx 40^\circ$ under the same conditions.

Let us consider light propagation through an optical fiber placed into longitudinal magnetic field in detail. Following the paper (Baranova & Zel'dovich, 1994) let us suppose that longitudinal magnetic field influences the propagation constant of only modes which retain their circular polarization and the change of the propagation constant value is $\delta\beta = -\sigma VHz$. Using Eq. (22) and Eq. (23) one can obtain the dependence of the fields $\mathbf{E}^-(r, \varphi, z, H)$ and

$\mathbf{E}^+(r, \varphi, z, H)$ on the magnetic field in the following form:

$$\begin{aligned} \mathbf{E}^+(r, \varphi, z, H) = & \\ & \frac{1}{\sqrt{2}} \cdot \begin{pmatrix} 1 \\ +i \end{pmatrix} \cdot \left\{ \sum_{m \neq 1} \sum_N B_{m,N} e^{-im(\varphi + VHz/m)} F_{m,N}(r) e^{iz(\beta_{m,N} + \delta\beta_{m,N}^{(2)})} \right. \\ & + \sum_{m \neq N} \sum_N A_{m,N} e^{+im(\varphi - VHz/m)} F_{m,N}(r) \exp \left[iz \left(\beta_{m,N} + \delta\beta_{m,N}^{(1)} \right) \right] \\ & \left. + e^{-i\varphi} \sum_N B_{1,N} F_{1,N}(r) e^{iz\beta_{1,N}} \left(e^{iz\delta\beta_{1,N}^{(2)}} + 1 \right) \right\} \\ & + \frac{1}{\sqrt{2}} \cdot \begin{pmatrix} 1 \\ -i \end{pmatrix} \cdot \left[e^{i\varphi} \sum_N B_{1,N} F_{1,N}(r) e^{iz\beta_{1,N}} \left(e^{iz\delta\beta_{1,N}^{(2)}} - 1 \right) \right], \end{aligned} \quad (34)$$

$$\begin{aligned} \mathbf{E}^-(r, \varphi, z, H) = & \\ & \frac{1}{\sqrt{2}} \cdot \begin{pmatrix} 1 \\ -i \end{pmatrix} \cdot \left\{ \sum_{m \neq 1} \sum_N A_{m,N} e^{+im(\varphi + VHz/m)} F_{m,N}(r) e^{iz(\beta_{m,N} + \delta\beta_{m,N}^{(2)})} \right. \\ & + \sum_{m \neq N} \sum_N B_{m,N} e^{-im(\varphi - VHz/m)} F_{m,N}(r) \exp \left[iz \left(\beta_{m,N} + \delta\beta_{m,N}^{(1)} \right) \right] \\ & \left. + e^{+i\varphi} \sum_N A_{1,N} F_{1,N}(r) e^{iz\beta_{1,N}} \left(e^{iz\delta\beta_{1,N}^{(2)}} + 1 \right) \right\} \\ & + \frac{1}{\sqrt{2}} \cdot \begin{pmatrix} 1 \\ +i \end{pmatrix} \cdot \left[e^{-i\varphi} \sum_N A_{1,N} F_{1,N}(r) e^{iz\beta_{1,N}} \left(e^{iz\delta\beta_{1,N}^{(2)}} - 1 \right) \right]. \end{aligned} \quad (35)$$

It can be seen from the expressions (34) and (35) that the case, when the circular polarization of the light at the input and output of the fiber is different, special, namely, the magnetic field does not influence the intensity distribution at the fiber output. This situation can be used for experimental verification of the adequacy of the used model. If the circular polarization at the input and output of the fiber has the same sign, the magnetic field will influence a speckle pattern at the fiber output.

The analysis of the expressions (34) and (35) shows that the modal structure of the radiation, propagating through a fiber, influences the behavior of the speckle pattern in the magnetic field. The angle of the speckle pattern rotation described by the expressions (34) and (35) is determined by the factors $\exp[+m(\varphi - VHz/m)]$ and $\exp[-m(\varphi + VHz/m)]$. These expressions show that the increase of the number of a mode results in the decrease of the angle of the speckle pattern rotation. The different angular contribution of the modes of different orders should result in such change of the speckle pattern which cannot be regarded as rotation. It means, that the rotation of the speckle pattern in a magnetic field should be manifested well in fibers which retain modes of the lowest orders, for such a case we shall consider the situation when the input light is linearly polarized, and the output linearly polarized light has the same azimuth of polarization. Let's consider the influence of a magnetic field on linearly polarized light propagating through a few modes optical fiber

retaining only modes with $m = 0$ and $m = 1$. Suppose that $N = 1$ and omit the coefficient N . Let the linearly polarized radiation at the fiber input be polarized along the x -axis, and the linearly polarized radiation at the fiber output have the same azimuth of polarization, then the amplitude of the field of the light wave E_x^x at the fiber output will look like the following:

$$\begin{aligned} \mathbf{E}_x^x(r, \varphi, z, H) = & \\ & \frac{1}{\sqrt{2}} \cdot F_0(r) e^{iz(\beta_0 + \delta\beta_0^{(1)})} (A_0 + B_0) (e^{-iVHz} + e^{iVHz}) \\ & + \frac{1}{\sqrt{2}} \cdot F_1(r) e^{iz\beta_1} \left[e^{iz\delta\beta_1^{(1)}} (A_1 e^{+i(\varphi - VHz)} + B_1 e^{-i(\varphi - VHz)}) \right. \\ & \quad \left. + (e^{iz\delta\beta_1^{(2)}} + 1) (A_1 e^{+i\varphi} + B_1 e^{-i\varphi}) \right] \\ & + \frac{1}{\sqrt{2}} \cdot F_1(r) e^{iz\beta_1} (e^{iz\delta\beta_1^{(2)}} - 1) (A_1 e^{-i\varphi} + B_1 e^{i\varphi}). \end{aligned} \quad (36)$$

In the simplest special case, when $A_0 = B_0 = 0$ and $A_1 = B_1 = A$ the expression (36) becomes:

$$\mathbf{E}_x^x(r, \varphi, z, H) = A\sqrt{2}F_1(r)e^{iz\beta_1} \left(e^{iz\delta\beta_1^{(1)}} \cos(\varphi - VHz) + 2e^{iz\delta\beta_1^{(2)}} \cos\varphi \right). \quad (37)$$

As it follows from the expression (37), even in the simplest case which is difficult to implement experimentally, the rotation of the speckle pattern under the magnetic field change will be observed on some steady background which is determined by the length of the fiber. It means that the best conditions of a speckle pattern observation are determined not only by the mode structure of the radiation propagating through a fiber, but also by the fiber length.

The light intensity at the fiber output is the following:

$$\begin{aligned} I_x^x(r, \varphi, z, H) = |E_x^x(r, \varphi, z, H)|^2 = & \\ = |A|^2 F_1^2(r) (5 + \cos(2\varphi - 2VHz)) + & \\ + |A|^2 F_1^2(r) \left(2 \cos \left(z \left(\delta\beta_1^{(2)} - \delta\beta_1^{(1)} \right) \right) \right) (\cos(VHz) + \cos(2\varphi - VHz)) + \cos 2\varphi. \end{aligned} \quad (38)$$

It is possible to group together the terms in the expression (38) on their dependence on the variables r , φ , z and H :

$$I_x^x(r, \varphi, z, H) = I_1^{xx}(r, \varphi, z) + I_2^{xx}(r, z, H) + I_3^{xx}(r, \varphi, z, H) + I_4^{xx}(r). \quad (39)$$

Only the third term $I_3^{xx}(r, \varphi, z, H)$ in Eq. (39) depends on the magnetic field and influences the angular distribution of the intensity at the fiber output. Let us consider this term in detail:

$$I_3^{xx}(r, \varphi, z, H) = |A|^2 F_1^2(r) I_3^{xx}(\varphi, z, H). \quad (40)$$

Here

$$I_3^{xx}(\varphi, z, H) = D(z) \cos(2\varphi + \gamma(z, H)), \quad (41)$$

where

$$D(z, H) = \sqrt{1 + C(z)^2 + 2C(z) \cos(VHz)}, \quad (42)$$

$$C(z) = 2 \cos \left(z \left(\delta\beta_1^{(2)} - \delta\beta_1^{(1)} \right) \right) \quad (43)$$

and

$$\tan \gamma(z, H) = -\frac{\sin(2VHz) + C(z) \sin(VHz)}{\cos(2VHz) + C(z) \cos(VHz)}. \quad (44)$$

It follows from the expression (41) that the speckle pattern rotation under the magnetic field influence will be determined by the angle $\gamma(z, H) / 2$. In the approach $VHz \ll 1$ it is possible to present the expression (44) as follows:

$$\tan \gamma(z, H) \approx -\frac{VHz(2 + C(z))}{1 + C(z)}. \quad (45)$$

Thus, it follows from the expression (45) that under the considered approach the angle of rotation linearly depends on the value of the applied field at the given length of the fiber. Dependence of the rotation angle on the length of the fiber at a specified value of a magnetic field has a nonlinear character. The linear dependence is possible in two cases, when $C(z) \ll 1$ or $C(z) \gg 1$. The function $C(z)$ is periodic and varies in the range from -2 up to $+2$, therefore, linear dependence of the rotation angle on the length of the fiber is possible only in a narrow range of lengths of the fiber.

Eqs. (34) and (35) were used for numerical modeling. The following parameters of an optical fiber with a step like refractive index profile were used: $n_{co} = 1.47$, $\Delta n = 0.004$ and $\rho = 4.5 \mu\text{m}$. The Verdet constant V was accepted to be equal to $V = 1.4 \cdot 10^{-2} \text{ min}/(\text{Gs} \cdot \text{cm})$. The coefficients in the expressions (34) and (35) were chosen by means of the random number generator. Calculation was carried out for different states of polarization at the fiber input and output, it was revealed that the state of polarization plays the important role only in one, the above-stated case. In Fig. 14 the calculated dependences of the angle of rotation of the

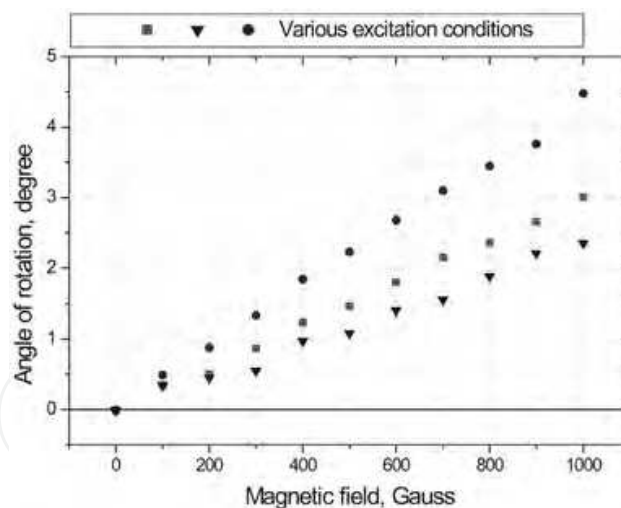


Fig. 14. Dependence of the angle of the speckle rotation on the value of a magnetic field at a different mode structure of radiation, the total length of the fiber $L = 100 \text{ cm}$, the length of the fiber in the field $L_{mf} = 23 \text{ cm}$.

speckle pattern of light passed through an optical fiber placed in a longitudinal magnetic field at the change of a direction of a magnetic field on the magnetic field value are presented. Figure 14 shows that the angle of rotation of the speckle pattern of light propagating in a few modes fiber placed in a longitudinal magnetic field linearly depends on the value of the applied magnetic field, however, the angle of rotation at the fixed value of the magnetic field depends on the mode structure of the radiation propagating through the fiber.

The experimental research of the propagation of the polarized radiation in a few modes germanosilicate optical fiber was carried out using a fiber with the following parameters: the difference of the refractive indexes of the core and the cladding $\delta n = 0.004$, the diameter of the core of the fiber $\rho = 4.5 \mu\text{m}$. A He-Ne laser was used as the radiation source, the experimental setup allowed to replace this laser with another one radiating at a required wavelength. For the analysis of obtained images of speckle patterns (for the demonstration of an angle of rotation) the special software for computer image processing was developed which allowed to compare two images, to determine the angle of mutual rotation with high accuracy and also the degree of identity of two images. The special software was used for processing both the experimental results and the results of the computer simulation. Images of speckle patterns of the radiation with the wavelength $\lambda = 633 \text{ nm}$ propagating in the same a few mode germanosilicate optical fiber placed in the longitudinal magnetic field of the value 500 Gs are presented in Fig. 15. The images were registered under opposite directions of

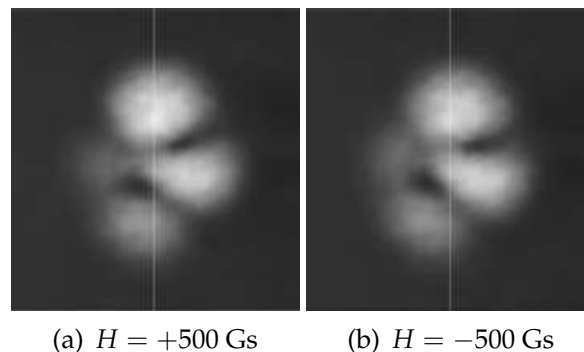


Fig. 15. images of the speckle patterns of the radiation with the wavelength $\lambda = 633 \text{ nm}$ propagating in a few modes germanosilicate optical fiber placed in the longitudinal magnetic field of the value 500 Gs at the opposite directions of the magnetic field.

the magnetic field. The speckle pattern is practically unchanged, and the visual observation confirms the presence of the rotation.

However, the change of the conditions of the radiation input has shown that the change of the mode structure can result in a significant speckle pattern change under the change of the magnetic field direction, but this change is not characterized by rotation. To investigate the influence of the magnetic field on the speckle pattern rotation under different conditions, the conditions for input of the He-Ne laser radiation were chosen such that provided the speckle pattern change of the rotation type. Dependence of the rotation angle of the speckle pattern of the radiation of the He-Ne laser passed through the germanosilicate optical fiber placed in the longitudinal magnetic field on the value of the magnetic field is presented in Fig. 16. One can see in Fig. 16 that the angle of rotation of the speckle pattern is linearly dependent on the value of the applied magnetic field. The investigation has shown that the change of the mode structure of the radiation propagating through the fiber results in the change of the slope of the linear dependence, however, the angle of rotation always was less than the Faraday angle.

The influence of a state of polarization at the fiber input and output on the behavior of the speckle pattern in the magnetic field was studied. It is revealed that generally the state of polarization does not influence the behavior of the speckle pattern under the change of the direction of the magnetic field. Essentially the other situation is observed in the case when circular polarization at the fiber input and output has opposite sign. According to the

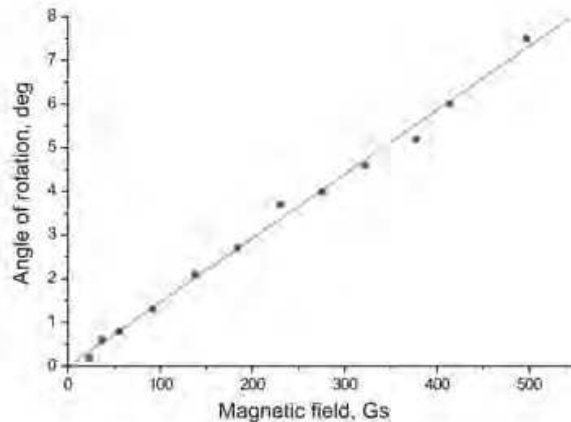


Fig. 16. Dependence of the rotation angle of the speckle pattern of radiation passed through the germanic silicate optical fiber placed in the longitudinal magnetic field on the value of the magnetic field. Length of the fiber in the magnetic field is 90 cm.

theoretical predictions no change of the speckle pattern at the change of the magnetic field direction was observed under any conditions of radiation input into the fiber.

The results of the investigations carried out for germanosilicate fibers, along with the comparison of the theoretical and experimental results, allow to conclude that the magnetic rotation of the speckle pattern of the light transmitted through an optical fiber placed in a longitudinal magnetic field will be best observed in optical fibers which keep only modes of the two lowest orders. The values of the magnetic field H , the Verdet constant V , and the fiber length in the magnetic field z should be such that $VHz \ll 1$.

7. Applications for fiber sensors

The analysis of the Eqs. (34) and (35) shows that modal structure of the radiation, propagating through a fiber, influences the behavior of the speckle pattern in the magnetic field. The angle of rotation of the speckle pattern described by the expressions (34) and (35) is determined by the factors $\exp [+m(\varphi - VHz/m)]$ and $\exp [-m(\varphi + VHz/m)]$. The speckle pattern rotation angle is determined by superposition of the rotation angles of all the modes. The angular intensity profile in a given crosssection of each mode is determined by the factor

$$\delta\varphi = \pm VHz/m. \quad (46)$$

Equation (46) shows that the increase of the number of a mode results in the decrease of the angle of the speckle pattern rotation. Thus, the different angular contribution of the modes of different orders should result in such change of the speckle pattern which cannot be regarded as rotation.

Figure 17 and Fig.18 show the images of the speckle patterns calculated using Eqs. (34) and (35) for the fiber with $\rho_0 = 4.5 \mu\text{m}$, $N_A = 0.11$, $n_{co} = 1.47$, and the fiber length in the magnetic field $L_{mf} = 20 \text{ cm}$ for the light wavelength $\lambda = 0.532 \mu\text{m}$ and the magnetic field strength $H = 1000 \text{ Gs}$. The calculations were performed for the case when all the modes that can be excited at the given wavelength propagate through the fiber and for the case when only modes with $m = 0$ and $m = 1$ propagate through the fiber. As can be seen in Fig. 17 an Fig.

18, the speckle pattern is distorted when the magnetic field is switched on, but when only the modes with $m = 0$ and $m = 1$ propagate, the speckle pattern is rotated.

It can be expected that the distortion of the speckle pattern will be proportional to the magnetic field strength. To prove this hypothesis, the dependencies of the speckle pattern rotation angle and the rms deviation of two speckle patterns on the magnetic field strength have been calculated for the case when only the modes with $m = 0$ and $m = 1$ are retained in the fiber and for the case when all possible fiber modes propagate. The results of calculations for the fiber with the same parameters ($\rho_0 = 4.5 \mu\text{m}$, $N_A = 0.11$, $n_{\text{co}} = 1.47$, $L_{\text{mf}} = 20 \text{ cm}$, $\lambda = 0.532 \mu\text{m}$) are shown in Fig. 19. It can be seen in Fig. 19 that, for the case when pure rotation of the speckle pattern in the fiber can be observed, the angle of rotation of the speckle pattern and the rms deviations of the speckle pattern obtained at $H = 0$ and $H \neq 0$ vary linearly with the magnetic field strength, though the slopes of these two straight lines are different. When all modes propagate in the fiber and only the distortion of the speckle pattern can be observed, the rms deviations of the speckle patterns obtained at $H = 0$ and $H \neq 0$ also vary linearly with the magnetic field strength; however, the slope of the line is smaller than in the case when only modes with $m = 0$ and $m = 1$ are retained in the fiber. Thus, to detect changes in the magnetic field strength, one can use both the dependence of the speckle pattern rotation

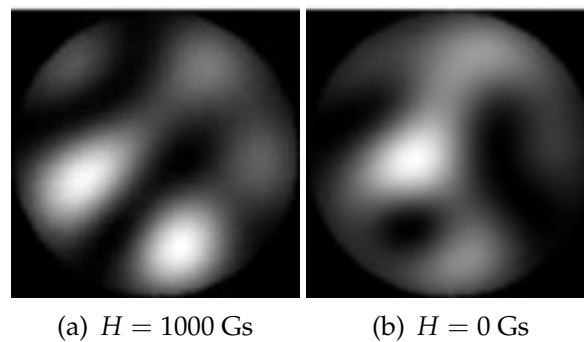


Fig. 17. Calculated intensity distribution in speckle pattern of light transmitted through optical fiber with $\rho_0 = 4.5 \mu\text{m}$, $N_A = 0.11$, $n_{\text{co}} = 1.47$, length of the fiber in magnetic field $L_{\text{mf}} = 20 \text{ cm}$, $\lambda = 0.532 \mu\text{m}$ for the case when all the modes that can propagate in the fiber are taken into account at $H = 0$ and $H = 1000 \text{ Gs}$.

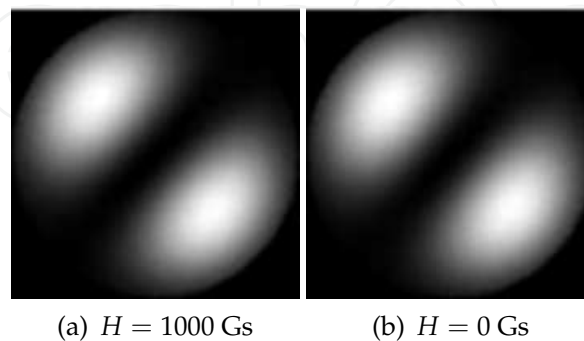


Fig. 18. Calculated intensity distribution in speckle pattern of light transmitted through optical fiber with $\rho_0 = 4.5 \mu\text{m}$, numerical aperture $N_A = 0.11$, $n_{\text{co}} = 1.47$, length of the fiber in magnetic field $L_{\text{mf}} = 20 \text{ cm}$, $\lambda = 0.532 \mu\text{m}$ for the case when only the modes with $m = 0$ and $m = 1$ are considered at $H = 0$ and $H = 1000 \text{ Gs}$.

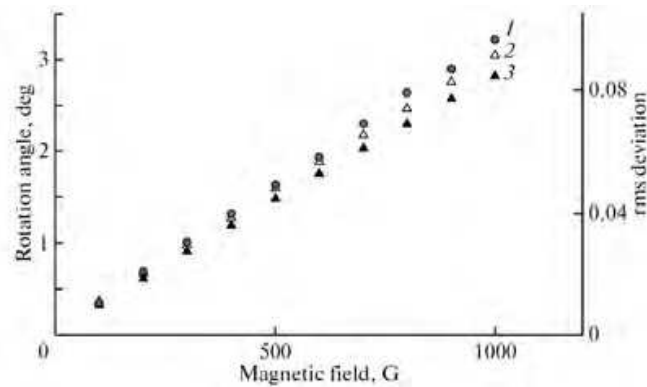


Fig. 19. Dependence of speckle pattern rotation angle (1) and rms deviation (2, 3) of the two speckle patterns obtained at $H = 0$ and $H \neq 0$ on magnetic field strength for cases when only modes with $m = 0$ and $m = 1$ are retained in the fiber (1 and 2) and when all possible modes propagate in the fiber (3).

angle on the magnetic field strength and the dependence of the rms deviation of the speckle pattern on the magnetic field strength.

Changes in the speckle pattern can be easily detected by means of a CCD camera and a computer. However, this method of detection is not suitable for detecting changes in the speckle pattern caused by rapidly varying or pulsed magnetic fields. As a promising method of detecting changes in the speckle pattern, the method of recording dynamic holograms in photorefractive crystals may be considered (Zel'dovich et al., 1995).

Let us consider the records and reconstruction of holograms in a photorefractive crystal by an inhomogeneous light field (by a speckle pattern). The hologram of interference between the signal beam (speckled field) and the reference Gauss beam is written in the photorefractive crystal in the absence of the magnetic field. The signal beam is a speckled light field transmitted through the optical fiber. If the reference beam is blocked after the hologram has been written, then the signal beam illuminating the photorefractive crystal will restore the Gaussian beam. The influence of the magnetic field results in the speckle pattern distortion. Under these conditions, the intensity of the restored Gaussian beam decreases in proportion with the degree of the speckle pattern distortion and, hence, in proportion with the magnetic field strength.

A few mode optical fiber with a step like refractive index profile was used for experimental investigation. The length of the fiber is 36 cm, $\rho_0 = 4.5 \mu\text{m}$, $n_{\text{co}} = 1.47$ and $N_A = 0.11$. A photorefractive crystal of barium-sodium niobate $\text{Ba}_2\text{NaNb}_5\text{O}_{15}$ (BNN), $3.5 \times 5.0 \times 7.5 \text{ mm}^3$ in size was used as a nonlinear medium for recording dynamic hologram. The pulsed magnetic field was produced by a solenoid. A beam of laser operated at a wavelength $\lambda = 0.532 \mu\text{m}$ was used. The intensity of the diffracted beam was detected upon excitation of different modes in the optical fiber, i.e., at different kinds of the speckle pattern at the fiber end. Figure 20 shows the experimentally obtained dependence of the reconstructed Gauss beam intensity on the value of magnetic field on the solenoid axis. It can be seen in Fig. 20 that the reconstructed Gauss beam intensity depends on the value of magnetic field linearly. It means that the form of the pulse magnetic field can be easily determined.

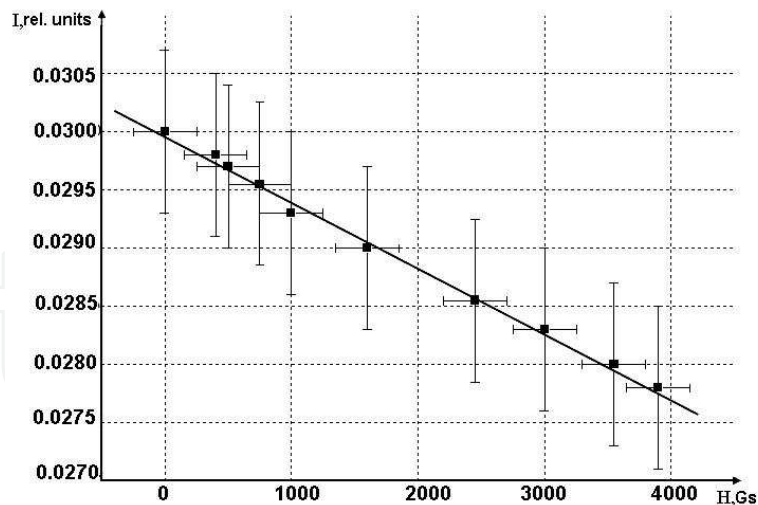


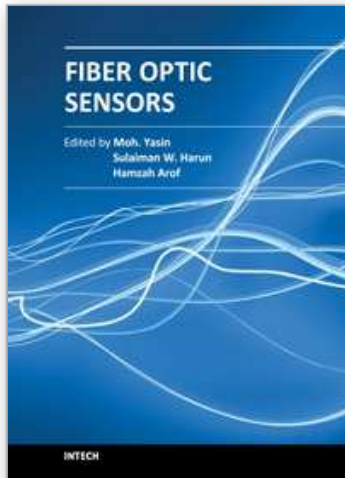
Fig. 20. The dependence of the reconstructed beam intensity on the value of magnetic field on the solenoid axis.

As a result, the usage of the effect of distortion of the speckle pattern of the light transmitted by the optical fiber in an external longitudinal magnetic field in combination with dynamic holography of the speckle fields can be used to detect the magnetic field pulse shape.

8. References

- Anikeev, V. V., Bolshakov, M. V., Kundikova, N. D., Valeev, A. I. & Zinatulin, V. S. (2001). The influence of a magnetic longitudinal field on the behavior of the speckle-pattern of the light, transmitted through optical fiber, *XVII International Conference on Coherent and Nonlinear Optics, "ICONO 2001"*, Technical Digest, Minsk, Belarus.
- Ardasheva, L. I., Sadykova, M. O., Sadykov, N. R., Chernyakov, V. E., Anikeev, V. V., Bolshakov, M. V., Valeev, A. I., Zinatulin, V. S. & Kundikova, N. D. (2002). Rotation of the speckle pattern in a low-mode optical fiber in a longitudinal magnetic field, *J. Opt. Technol.* 69: 10–15.
- Azzam, R. M. A. & Bashara, N. M. (1977). *Ellipsometry and polarized light*, North - Holland Publishing Company, New York.
- Baranova, N. B. & Zel'dovich, B. Y. (1994). Rotation of a ray by a magnetic field, *JETP Lett.* 59: 681–684.
- Bolshakov, M. V., Ershov, A. V. & Kundikova, N. D. (2008). Fiber-optic system for magnetic field change registration, *International Commission for Optics ICO 21 Ú 2008 Congress Optics for the 21 st Century*, Book of Proceeding, Sydney, Australia, p. 286.
- Bolshakov, M. V., Ershov, A. V. & Kundikova, N. D. (2011). Optical method for detecting variations of the magnetic field strength, *Optics and Spectroscopy* 110: 624–629.
- Bolshakov, M. V. & Kundikova, N. D. (2003). The influence of the light polarization state on the speckle pattern of light transmitted through a fiber, *Proceedings of the Chelyabinsk scientific center* 4: 26–31.
- Bolshakov, M. V., Vaganova, N. S. & Kundikova, N. D. (2006). Experimental investigation of the coherent light propagation with the arbitrary polarization state through an optical fiber, *Proceedings of the Chelyabinsk scientific center* 1: 10–15.
- Chiao, R. Y. & Wu, Y.-S. (1986). Manifestations of berry's topological phase for the photon, *Phys. Rev. Lett.* 57: 933–936.

- Darsht, M. Y., Zel'dovich, B. Y., Kataevskaya, I. V. & Kundikova, N. D. (1995). Formation of single wave front dislocation, *JETP* 107: 1464–1472.
- Darsht, M. Y., Zel'dovich, B. Y., Zhirgalova, I. V. & Kundikova, N. D. (1994). Observation of a "magnetic rotation" of the speckle of light passed through an optical fiber, *JETP Lett.* 59: 763–765.
- Doogin, A. V., Kundikova, N. D., Liberman, V. S. & Zel'dovich, B. Y. (1992). Optical magnus effect, *Phys. Rev. A* 45: 8204–8208.
- Doogin, A. V., Zel'dovich, B. Y., Kundikova, N. D. & Liberman, V. S. (1991). The influence of circular polarization on light propagation in optical fiber, *JETP Lett.* 53: 186–188.
- Fedorov, F. I. (1955). On the theory of total internal reflection, *Dokl. Akad. Nauk SSSR* 105(5): 465–469.
- Gerrard, A. & Burch, J. M. (1975). *Introduction to matrix methods in optics*, John Wiley and sons, New York.
- Goltser, I. V., Darsht, M. Y., Kundikova, N. D. & Zel'dovich, B. Y. (1993). An adjustable quarter-wave plate, *Optics Communications* 97: 291–294.
- Goos, F. & Hanchen, H. (1947). Ein neuer und fundamentaler versuch zur totalreflexion, *Ann. Physik.* 436(7-8): 333–346.
- Goos, F. & Hanchen, H. (1949). Neumessung des strahlversetzungseffektes bei totalreflexion, *Ann. Physik.* 440(3-5): 251–252.
- Imbert, C. (1972). Calculation and experimental proof of the transverse shift induced by total internal reflection of a circularly polarized light beam, *Phys. Rev. D.* 5: 787–796.
- Picht, J. (1929). Beitrag zur theorie der totalreflexion, *Ann. Physik.* 395(4): 433–496.
- Rytov, S. M. (1938). On transition from wave to geometrical optics, *Dokl. Akad. Nauk SSSR* 18: 263–266.
- Snyder, A. W. & Love, J. D. (1984). *Optical Waveguide Theory*, Methuen, London.
- Tomita, A. & Chiao, R. Y. (1986). Observation of berry's topological phase by use of an optical fiber, *Phys. Rev. Lett.* 57: 937–940.
- Vladimirskii, V. V. (1941). The rotation of a polarization plane for curved light ray, *Dokl. Akad. Nauk SSSR* 21: 222–225.
- Zel'dovich, B. Y., Kataevskaya, I. V. & Kundikova, N. D. (1996). Inhomogeneity of the optical magnus effect, *Quantum Electron* 26: 87 – 88.
- Zel'dovich, B. Y. & Liberman, V. S. (1990). Rotation of the plane of a meridional beam in a graded-index waveguide due to the circular nature of the polarization, *Quantum Electronics* 20: 427–428.
- Zel'dovich, B. Y., Mamaev, A. V. & Shkunov, V. V. (1995). *Speckle-Wave Interactions in Application to Holography and Nonlinear Optics*, CRC Press.



Fiber Optic Sensors

Edited by Dr Moh. Yasin

ISBN 978-953-307-922-6

Hard cover, 518 pages

Publisher InTech

Published online 22, February, 2012

Published in print edition February, 2012

This book presents a comprehensive account of recent advances and researches in fiber optic sensor technology. It consists of 21 chapters encompassing the recent progress in the subject, basic principles of various sensor types, their applications in structural health monitoring and the measurement of various physical, chemical and biological parameters. It also highlights the development of fiber optic sensors, their applications by providing various new methods for sensing and systems, and describing recent developments in fiber Bragg grating, tapered optical fiber, polymer optical fiber, long period fiber grating, reflectometry and interferometry based sensors. Edited by three scientists with a wide knowledge of the field and the community, the book brings together leading academics and practitioners in a comprehensive and incisive treatment of the subject. This is an essential reference for researchers working and teaching in optical fiber sensor technology, and for industrial users who need to be aware of current developments and new areas in optical fiber sensor devices.

How to reference

In order to correctly reference this scholarly work, feel free to copy and paste the following:

Maxim Bolshakov, Alexander Ershov and Natalia Kundikova (2012). Optical Effects Connected with Coherent Polarized Light Propagation Through a Step-Index Fiber, *Fiber Optic Sensors*, Dr Moh. Yasin (Ed.), ISBN: 978-953-307-922-6, InTech, Available from: <http://www.intechopen.com/books/fiber-optic-sensors/optical-effects-connected-with-coherent-polarized-light-propagation-through-a-step-index-fiber>

INTECH
open science | open minds

InTech Europe

University Campus STeP Ri
Slavka Krautzeka 83/A
51000 Rijeka, Croatia
Phone: +385 (51) 770 447
Fax: +385 (51) 686 166
www.intechopen.com

InTech China

Unit 405, Office Block, Hotel Equatorial Shanghai
No.65, Yan An Road (West), Shanghai, 200040, China
中国上海市延安西路65号上海国际贵都大饭店办公楼405单元
Phone: +86-21-62489820
Fax: +86-21-62489821

© 2012 The Author(s). Licensee IntechOpen. This is an open access article distributed under the terms of the [Creative Commons Attribution 3.0 License](#), which permits unrestricted use, distribution, and reproduction in any medium, provided the original work is properly cited.

IntechOpen

IntechOpen